Erschienen in: Nanoscale ; 9 (2017), 23. - S. 7868-7874
https://dx.doi.org/10.1039/c7nr01874f

Near-equilibrium measurement of quantum size effects using Kelvin probe force microscopy

Thomas Späth, ‡ Matthias Popp, Carmen Pérez León, * Michael Marz and Regina Hoffmann-Vogel§

In nano-structures such as thin films electron confinement results in the quantization of energy levels in the direction perpendicular to the film. The discretization of the energy levels leads to the oscillatory dependence of many properties on the film thickness due to quantum size effects. Pb on Si(111) is a specially interesting system because a particular relationship between the Pb atomic layer thickness and its Fermi wavelength leads to a periodicity of the oscillation of two atomic layers. Here, we demonstrate how the combination of scanning force microscopy (SFM) and Kelvin probe force microscopy (KPFM) provides a reliable method to monitor the quantum oscillations in the work function of Pb ultra-thin film nano-structures on Si(111). Unlike other techniques, with SFM/KPFM we directly address single Pb islands, determine their height while suppressing the influence of electrostatic forces, and, in addition, simultaneously evaluate their local work function by measurements close to equilibrium, without current-dependent and non-equilibrium effects. Our results evidence even–odd oscillations in the work function as a function of the film thickness that decay linearly with the film thickness, proving that this method provides direct and precise information on the quantum states.

1 Introduction

Electrons in atomically flat metallic thin films located on surfaces with a band gap are confined in the potential well formed between the vacuum level and the substrate band gap. The confinement results in the quantization of the energy levels.[1–3] In thin film nano-structures, *i.e.* islands, the confinement of the electrons takes place in the *z*-direction perpendicular to the surface, leading to a pronounced effect of the quantization of the perpendicular wave-vector component k_z, while k_x and k_y remain quasi-continuous. Consequently, the Fermi sphere of allowed states is reduced to a discrete number of Fermi discs with a constant k_z value[1,4] (see Fig. 1a). If one were able to increase the film thickness continuously, the number of Fermi discs would grow and would move closer together in the reciprocal space[3] (see Fig. 1a). The periodic addition of Fermi discs results in oscillations of the Fermi energy (E_F) *i.e.* of the chemical potential, as a function of the film thickness.[4] As a consequence quantum size effects (QSE) lead to an oscillatory behavior of many physical and chemical properties as a function of the film thickness, such as the surface energy,[4] electric resistivity,[5] the superconducting critical temperature,[6,7] the surface chemical reactivity,[8,9] the work function and accordingly the chemical potential.[8,10,11] The work function is defined as $\Phi = E_{vac} - \mu$, E_{vac} being the energy of the vacuum level, and μ the chemical potential, see Fig. 1e. Typical systems where QSE have been observed are Ag/Au(111),[2] Ag/Fe(100),[3] Pb/Cu(111),[12] Pb/Ag(111),[13] and Pb/Si(111).[4,6–11,14–16] Among these systems, Pb on Si(111) has been intensely investigated, since it exhibits a rich variety of pronounced QSE.[17]

In Pb thin films, the Fermi energy remains pinned to one Fermi disc until the number of electrons exceeds the number of states available in that disc, then it jumps to the next one. This occurs with good approximation when the thickness of the film a reaches

$$a = n\frac{\lambda_F}{2}, \quad (1)$$

where λ_F is the Fermi wavelength that varies with the film thickness and n an integer number. The thickness of an

Physikalisches Institut, Karlsruhe Institute of Technology (KIT), Wolfgang-Gaede-Str. 1, 76128 Karlsruhe, Germany. E-mail: carmen.perez.leon@kit.edu

‡Present address: Department of Materials Science, Darmstadt University of Technology, Jovanka-Bontschits-Str. 2, 64287 Darmstadt, Germany.
§Present address: Institut für Angewandte Physik, Karlsruhe Institute of Technology (KIT), Wolfgang-Gaede-Str. 1, 76128 Karlsruhe, Germany.

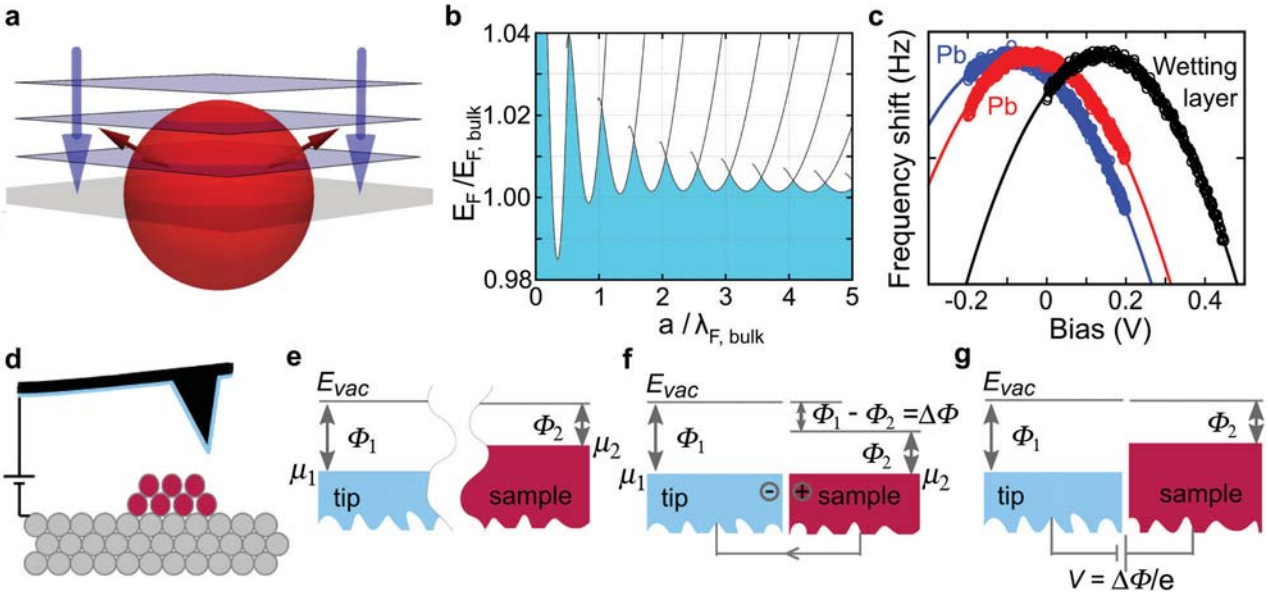

Fig. 1 Quantum size effects on thin metal films and fundamentals of the Kelvin method. (a) The Fermi sphere of allowed states is reduced to a discrete number of Fermi discs in k_z-direction (n = 2 in the sketch, see ESI Section I†). (b) Oscillation of the Fermi energy of a Pb(111) film with the film thickness. The depth of the potential well is $1.05E_{F,bulk}$, see ESI Section I.† (c) Kelvin parabolas measured on different parts of the sample: wetting layer, 7 and 8 atomic layers high Pb islands (blue and red curves, respectively) and fitting parabolas to the data. The curves have been adjusted vertically for clarity. (d) Sketch of tip and sample configuration. (e) Electronic energy levels of two materials at infinite distance from each other. (f) Charge transfer when the two materials are brought together. (g) Minimisation of electrostatic forces using the Kelvin method.

atomic Pb layer, d_0 = 0.285 nm,[18] satisfies approximately the relation

$$2d_0 \approx 3\frac{\lambda_{F,bulk}}{2}, \quad (2)$$

where $\lambda_{F,bulk}$ = 0.394 nm is the bulk Fermi wavelength of Pb.[18–20] Thus, if the film thickness is increased by two atomic layers, three states are added and the E_F remains nearly constant. If, however, the film is increased by just one atomic layer, only one state is added and there is a strong difference in E_F. This yields to oscillations of E_F and the work function with the film thickness. The amplitude of these oscillations decays as more and more Fermi discs become populated, *i.e.* the nano-structure gradually approaches bulk properties.[4] This behavior is shown in Fig. 1b, where the graph has been generated with a simple model described in the ESI Section I.† The oscillation with a wavelength of $\lambda_{F,bulk}/2$ is additionally modulated by a quantum beating pattern that causes a periodical reversal of maxima and minima.[19] This beating pattern results from the interference of the damped oscillations and the discrete nature of the atomic layer structure of the film.[4,19] As indicated in eqn (2), the relation is not exactly 3 but rather $2d_0 \approx 2.9\cdot(\lambda_{F,bulk}/2)$. Since the value 2.9 differs by 10% from the next integer 3, every ten atomic layers a phase slip is expected. The ultra-thin thickness limit of the first beating merits particular attention because in this regime the amplitude of the oscillations is the largest.[4,10,19,20]

In order to detect the quantum oscillations in the work function two approaches were applied in the past. One approach was photoemission.[2,17] Since this method integrates over a large surface area, it integrates over all film thicknesses present within this area. The main difficulty is to produce a large fraction of thin films with a homogeneous thickness on the one hand, and to interpret the integrated data on the other hand. Another approach was to address single islands, using scanning tunneling microscopy (STM) with a lock-in technique. This was achieved by measuring the tunneling current as a function of tip–sample distance and bias voltage. Following, the results were fitted to models including the work function.[8,10,11] This method led to contradictory results, because the oscillations observed using STM varied in phase depending on the bias voltage applied, an effect attributed to the electronic state the tunneling electrons occupy in the Pb island.[11]

Here, we show how simultaneous Kelvin probe force microscopy (KPFM, see ref. 21) and scanning force microscopy (SFM) assist in explaining these results by directly measuring the influence of QSE on the local work function (LWF) in ultra-thin Pb islands on Si(111). The main advantage of this method *vs.* STM is that the measurement of the LWF is carried out very close to equilibrium, since KPFM determines the LWF without extracting electrons, *i.e.* essentially without any current. Thus, we suppress current-dependent and non-equilibrium effects.

With KPFM, the work function difference between tip and sample, $\Delta\Phi$, is directly determined during SFM measurements (Fig. 1d). The microscope is operated in the dynamic frequency modulation mode, where the tip oscillates at its resonance fre-

quency, and the frequency shift of this oscillation is a measure of the tip–sample interaction, *i.e.* of the force between them. Since the tip–sample system acts as a capacitor with a capacitance C, applying a bias voltage V leads to parabolic force F between tip and sample,

$$F = \frac{1}{2}\frac{\partial C}{\partial z}\left(V - \frac{\Delta\Phi}{e}\right)^2, \quad (3)$$

where z is the tip–sample distance. The tip – Si or Pt/Ir-coated Si here – and the sample – Pb – have different WF (Fig. 1e). When the tip is approached to the sample, charge transfer between tip and sample leads to a shift of the parabola by $V = \Delta\Phi/e$, and the chemical potentials align (Fig. 1f). Fig. 1c shows the parabolic dependence of the frequency shift on the bias voltage measured on different parts of the sample (see eqn (3)). Applying a bias voltage between tip and sample that equals their WF difference, the Kelvin voltage ($V_{\mathrm{Kelvin}} = \Delta\Phi/e$), electrostatic forces between them are minimized (Fig. 1g). Assumptions about the shape of the potential well between tip and sample are not needed if the distance between tip and sample is large enough to avoid chemical bonding. At this distance range, the measured LWF does not depend on the tip–sample distance.[22] The KPFM measurements were performed in the range where the current flow was below the detection limit of our experimental setup.

2 Experimental section

2.1 Sample preparation

The n-type Si(111) crystals (phosphorous-doped, ρ = 7.5 Ω cm) were first shortly heated to 1200 °C in a commercial ultra-high vacuum chamber (Omicron Nano-Technology GmbH, Taunusstein, Germany) with a base pressure below 3×10^{-8} Pa. Prior to Pb evaporation, for some samples the Si(111) substrate was cooled down to room temperature, whereas for other samples the Si substrate was first cooled to liquid nitrogen temperatures and then annealed at room temperature for times between 20 and 40 min. After Pb deposition, the samples were transferred immediately to the liquid nitrogen pre-cooled scanning force microscope (Omicron VT-AFM) at ~110 K attached to the same vacuum vessel for the measurements. For more details on the Pb deposition see ESI Section II.†

2.2 Scanning force microscopy methods

For low temperature scanning force microscopy (SFM) imaging, we used commercial Si cantilevers (Nanosensors, Neuchâtel, Switzerland) with a spring constant of 30–60 N m^{-1} and resonance frequencies of approximately 300 kHz. The majority of the tips were coated with a 25 nm thick layer of Pt/Ir. The tips were first degassed in vacuum at 150 °C for several hours. Subsequently, they were cleaned by Ar sputtering. After sputtering the Pt/Ir tips remained highly conductive. The tips were transferred to the scanning force microscope located in the same vacuum vessel and tested on clean Si(111). The cantilever was oscillated at resonance at a constant amplitude of 5–10 nm. We used a Nanonis phase-locked loop electronics (SPECS, Zurich, Switzerland) to detect the frequency shift induced by the tip–sample interaction. We operated in the dynamic mode with frequency modulation technique (FM-SFM); this topographic detection mode is also called the non-contact mode. We performed Kelvin probe measurements in parallel to the topography measurements by applying an oscillating voltage to the tip with a typical frequency of f_{Kelvin} = 266 Hz and an amplitude of 0.5 V. Bias-dependent frequency shift measurements at different tip–surface distances within 1.7 nm from the surface showed neither a dependence of the Kelvin voltage on the distance nor a deviation from the parabolic shape. The sign of the measurement has been calibrated using a KBr(001) surface.[23] Negative charge accumulates on alkali halide crystals. We represent this negative charge by larger work function differences (bright contrast), *i.e.* higher Kelvin voltage. This convention was also double-checked on the Si(111)-(7 × 7) reconstructed part of a stepped Si (7 7 10) surface, where the negative charge expected on the restatoms was also correctly reproduced.[24] All SFM measurements were conducted at ~110 K.

3 Results and discussion

When a clean Si(111) surface is covered with small amounts of Pb, (111)-oriented islands grow following a Stranski–Krastanov growth mode surrounded by a disordered wetting layer (WL).[14,16,25] The islands with a flat-top mesa shape exhibit preferred heights influenced by the QSE.[14,16,25] At room temperature, thermally activated diffusion is strong and makes the islands grow with time. The islands' size can be controlled by varying the deposition parameters and annealing time. In previous STM studies, large Pb islands extending over many terraces were grown over stepped regions.[7–11] These flat-top mesas contained regions of different heights in one island owing to their stepped bottom surface. Our focus here is to concentrate on small islands covering only a few terraces, ideally only one. Thus, we avoid the influence of epitaxial strain of islands overgrowing many terraces due to the misfit of Pb(111) and Si(111) in the vertical direction.[8] We also aim at the limit of ultra-thin islands of only a few atomic layers in height, particularly below 10 atomic layers. In this height range, the amplitude of the quantum oscillations is the largest,[4,10,19,20] as we mentioned above, and the island height measurement particularly precise. Hence, after Pb deposition, we cooled down the sample to ~110 K by inserting it into the pre-cooled SFM to stop the diffusion process.

Fig. 2 shows SFM topographic and simultaneously obtained Kelvin images of ultra-thin Pb islands on Si(111). For an atomically resolved image of a Pb island, see Fig. S1 of the ESI.† The islands have a small lateral extension and heights in the desired range. The Kelvin images, Fig. 2b and d, confirm that the LWF differs for islands of different heights. As already noticed in Fig. 1c, also the LWF of the islands differs from the one of the WL. The lower Kelvin voltage

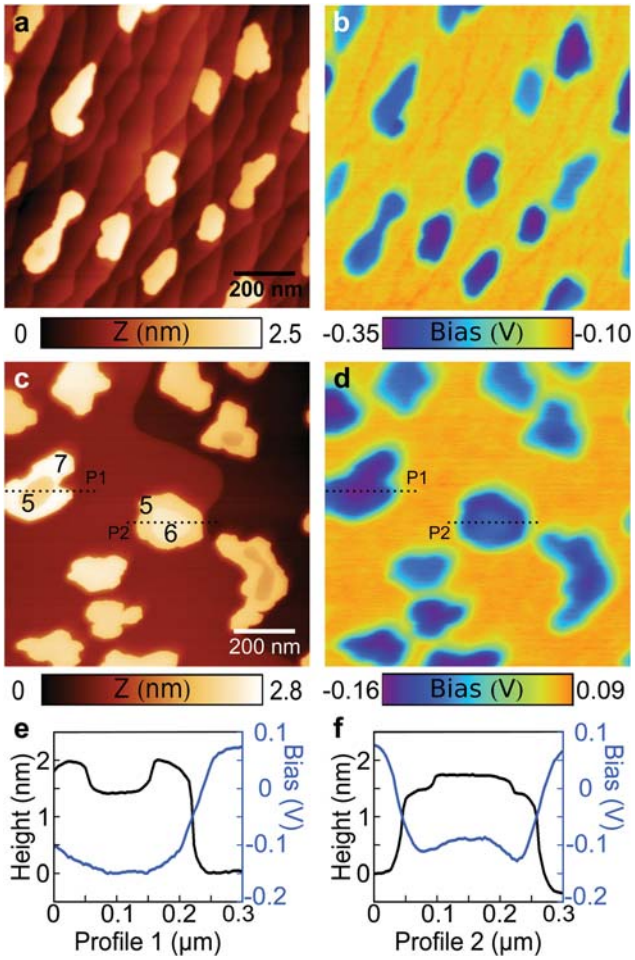

Fig. 2 SFM topographic (a, c) and simultaneously obtained Kelvin images (b, d) of ultra-thin Pb islands on Si(111). The numbers indicate the local height in atomic layers measured from the WL. (e, f) Profiles over Pb islands along the dashed lines marked in (c, d). Islands having internal height differences of one atomic layer show differing LWF within the island, while for internal height differences of two atomic layers the LWF is nearly equal over the whole island. This underlines the bilayer period of the quantum oscillation. Images size (1 × 1) μm^2; frequency shift (a, b) $\Delta f = -30$ Hz, (c, d) $\Delta f = -20$ Hz; oscillation amplitude (a, b) A = 5.3 nm, (c, d) A = 10 nm; normalized frequency (a, b) $\gamma = -2.1\,\mathrm{fN}\sqrt{\mathrm{m}}$, (c, d) $\gamma = -3.6\,\mathrm{fN}\sqrt{\mathrm{m}}$. Pt–Ir coated tips.

values on the islands indicate electron depletion with respect to the WL, following the description that higher Kelvin voltage implies more negative charge.[23,24,26] These results are in contrast to a previous SFM study that found no Kelvin voltage difference within a large Pb island with different heights.[27] That study used a tuning fork sensor with a higher stiffness and less sensitivity to the electrostatic force than the cantilevers used here.

In Fig. 2a, some islands cover more than one Si(111) terrace. Also on such islands regions with different heights show different work functions, as seen in Fig. 2b. In Fig. 2c, a few islands have a ring-like shape. In two of these ring-like shape islands in the middle of the image, the local island height measured from the WL is given in Pb atomic layers. These islands are particularly interesting, because they directly show the bilayer oscillation of the LWF on Pb islands.[15] For the 7 and 5 atomic layers high island, the whole island has a similar LWF, while for the 5 and 6 atomic layers high island, both parts display a strongly different LWF (see Fig. 2d, and profiles over the islands in Fig. 2e and f).

Another example of a Pb island covering several terraces is presented in Fig. 3. Unlike usual Pb islands on Si(111), this particular one does not have a mesa shape nor a ring-

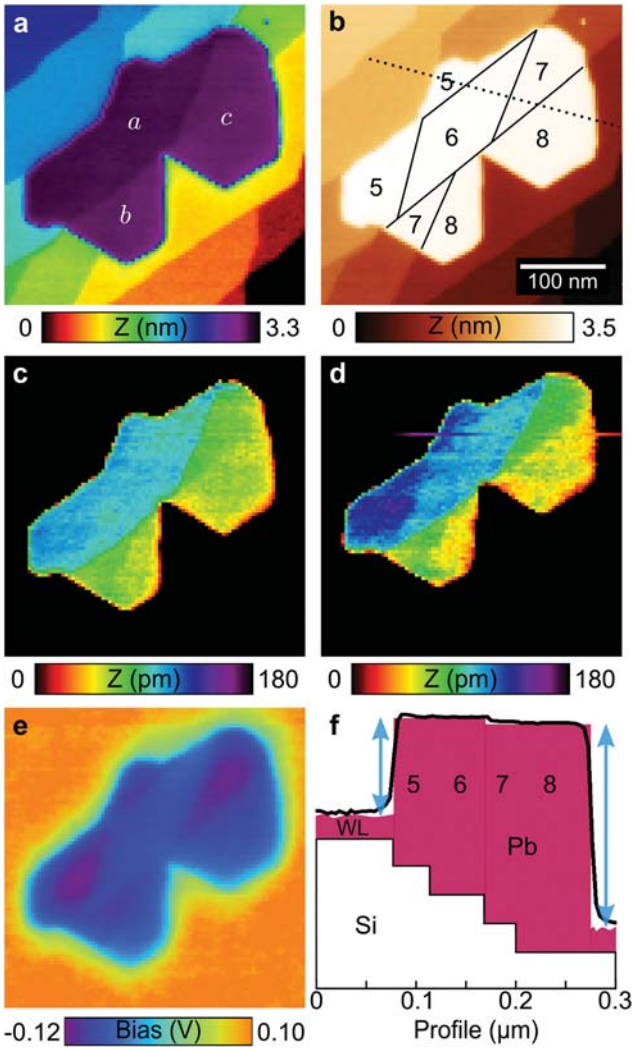

Fig. 3 SFM (a–d) and Kelvin (e) images of a Pb island composed of three flat-top small islands extending over several Si(111) terraces. The height of the island varies locally and consequently also the LWF. (a) Small islands labeled *a*, *b* and *c*. (b) Local height of the island given in atomic layers measured from the WL. (c) Topography obtained with the Kelvin controller switched on. (d) Topography obtained with the Kelvin controller switched off. The image is influenced by electrostatic forces. (e) Corresponding Kelvin voltage of image c. (f) Schematic cross section and profile of the island along the dashed line marked in (b). Image size (350 × 350) nm^2; frequency shift $\Delta f = -17$ Hz; oscillation amplitude A = 8 nm; normalized frequency $\gamma = -2.1\,\mathrm{fN}\sqrt{\mathrm{m}}$. Pt–Ir coated tip.

like shape but shows three different flat-top regions. These regions, as *a*, *b* and *c* in Fig. 3a, probably correspond to three coalescent smaller islands that merge to form a larger one.[28] These small flat-top islands, presumably single crystals, cover several terraces and therefore contain regions of different heights. The height in atomic layers (measured from the WL) of the distinct individual parts of the islands is indicated in Fig. 3b and f (5–8 atomic layers). Due to the misfit of Pb(111) and Si(111) in the vertical direction,[8] the *a* island slightly overtops the *b* and *c* ones, as observed in Fig. 3a. This height difference is noticeable as a step of sub-atomic height (~40 pm) in the profile shown in Fig. 3f. Owing to the rich morphology of this island, we have used it for investigating the influence of the QSE on SFM measurements.

SFM topographic imaging of the surface has been performed with the Kelvin controller switched on (Fig. 3c and e), and with the Kelvin controller switched off (Fig. 3d). The contrast is adjusted in the images to enhance the height differences. The topographic image in Fig. 3d obtained with the Kelvin controller switched off shows an island composed of many small fragments, these corresponding to the parts of the island indicated in Fig. 3b that cover different terraces. However in Fig. 3c imaged while minimizing electrostatic forces, the three flat-top regions that compose the island are well resolved. This demonstrates that the image in Fig. 3d was affected by electrostatic forces due to the strong variations of the LWF in the distinct parts of the islands, which are notably prominent in Fig. 3e.

It has been shown that to obtain reliable height measurements in samples with different materials or regions with differing electrostatic interactions the use of KPFM is mandatory.[29] Otherwise, the apparent height is strongly influenced by the tip–sample work function difference. Recent calculations have evidenced that owing to the QSE, electrostatic forces above islands are significant.[9] The quantization of the electronic states even influences the topographic STM measurement causing the imaging of buried inter-facial structures, that may mislead the interpretation of the topographic images of the islands.[10,30]

In Fig. 3c and e is also noticeable that for parts of the islands having an odd number of Pb layers from the WL, the local Kelvin voltage is significantly lower than in parts of the islands having an even number of atomic layers. This again evidences the bilayer oscillation of the LWF as a function of island height.

In order to address the quantum oscillations in the LWF of ultra-thin Pb islands on Si(111), we grew a large amount of small islands and investigated them with simultaneous SFM/KPFM, as in Fig. 2 and 3. The obtained data were analyzed by applying statistical methods that we detail in the ESI Section IV.† The particularity of our approach is that we use the WL as reference, instead of using the tip, the standard reference also in STM studies.[11] Consequently, in the analysis the height of the islands was measured from the WL. Likewise, we evaluated the LWF of the island in terms of the LWF of the WL. As we mentioned above, KPFM directly provides the work function difference between sample and tip:

$$e{\cdot}V_{\mathrm{Kelvin}} = \Delta\Phi = \Phi_{\mathrm{sample}} - \Phi_{\mathrm{tip}}. \tag{4}$$

Using the work function of the WL as reference:

$$\begin{aligned}\Delta\Phi^{*} &= e{\cdot}V_{\mathrm{Kelvin,island}} - e{\cdot}V_{\mathrm{Kelvin,WL}} \\ &= \Phi_{\mathrm{island}} - \Phi_{\mathrm{tip}} - (\Phi_{\mathrm{WL}} - \Phi_{\mathrm{tip}}) \\ &= \Phi_{\mathrm{island}} - \Phi_{\mathrm{WL}},\end{aligned} \tag{5}$$

we obtain tip-independent results. Since the LWF of the WL is homogeneous within the experiments shown here (see ESI Section V†), it only contributes as a constant offset.

Fig. 4 summarizes the evaluated data obtained with one single tip: the quantum oscillation of the LWF of Pb islands on Si(111) as a function of island height is directly obtained with SFM/KPFM. The amplitude of the oscillation decays for increasing island height, as expected. The advantage of using the WL as reference is that we can compare the results of different experiments directly. In Fig. S4 of the ESI† results obtained with diverse tips align well with each other, confirming that we indeed get tip-independent results. The relative change of the LWF from layer to layer, the phase of the beating pattern, and the decay of the oscillation are the most relevant quantities in this study, and these do not depend on the tip.

In the literature,[4,15,17,20] the damped sinusoidal function,

$$f(N) = \frac{A|\sin Nk_{\mathrm{F}}d_0 + \phi| + B}{N^{\alpha}} + C, \tag{6}$$

has been used to describe the periodicity and decay of the oscillation of the surface energy and work function as a function of the number of atomic layers *N*. In eqn (6), *A*, *B*, *C*, ϕ, and α are *N*-independent constants, and k_{F} is the Fermi wave vector measured from the zone boundary[20] (for details see ESI Section VI†). To evaluate the decay exponent of the oscillations, we have fitted this equation to our data. The values

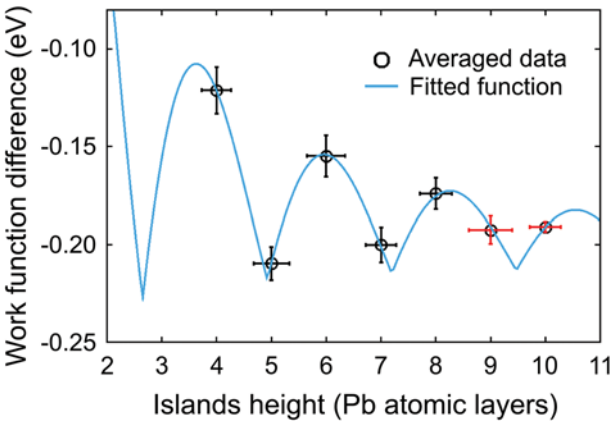

Fig. 4 Quantum oscillations in the local work function of ultra-thin Pb islands on Si(111) as a function of the island height measured from the WL obtained with SFM/KPFM. The LWF exhibits a damped even–odd oscillation with increasing island height. The two points with red error bars result from a small number of data. Data fitted with eqn (6).

obtained for the free parameters show that this description is suitable, see Table S1 of the ESI.† We find for the decay exponent α a value of 1.26. This value differs from the conventional $\alpha = 2$ of the Friedel oscillations in electron density at other metal surfaces,[31] we obtain also this value in the simple model described in the ESI Section I.† However, as stated in ref. 31, Fermi surface nesting leads to one-dimensional properties of the electrons in Pb(111) causing a deviation from simple physics that leads to a decay exponent $\alpha = 1$ for the work function.

In the introduction we announced the presence of a beating pattern. To study the behavior of the amplitude of the oscillations above 10 atomic layers, we grew larger islands (see details in ESI Section V†). Our results presented in Fig. S5† confirm a phase slip on the oscillations and show a knot around 9–10 atomic layers. Using these additional data, we fitted again α and obtained a value of 1.02 (see ESI Section VI†).

So far an analysis of the work function oscillation as a function of island height has been mainly performed using STM with a lock-in technique.[8,10,11] The oscillation has been observed and predicted up to an island height of 32 atomic layers.[10,18] It is difficult to compare our data with previous STM works, since the phase of the oscillation varies from publication to publication reversing minimum and maximum. This is partly due to different ways to count the number of atomic layers, *e.g.*, including or excluding the WL which is generally agreed to be around 1 atomic layer thick.[16,32] Another reason is the dependence of the STM-obtained LWF on the tunneling voltages used, as we mentioned above.[11,13] The maximum relative change from layer to layer in our SFM/KPFM studies is of 0.08–0.05 eV, whereas in the literature for islands above 10 atomic layers, this change is of 0.2–0.15 eV,[8,10] although a smaller value is expected due to the decay of the oscillation. An additional point to compare with is the thickness at which the knot of the beating pattern occurs, *i.e.* the phase of the beating. Some authors observe the first knot around 9–10 atomic layers,[8,10] like we do here, while others observe it at around 12–13 atomic layers.[11] This difference is hardly expected to be caused by different ways of counting the atomic layers or to imprecision by measuring the height. A possibility that may explain such difference could be differences in the metal–semiconductor interface that modify the position of the knots.[32–35]

4 Conclusions

Summarising, we have demonstrated that the SFM/KPFM combination provides a reliable method for measuring the influence of QSE on the work function of metallic ultra-thin films. The advantages of this technique *vs.* previous approaches is that we address single films and unambiguously determine their local thickness by suppressing the influence of the QSE on the topographic measurements, while simultaneously evaluating their LWF by measurements close to equilibrium, *i.e.* essentially without any current. In addition, in our study we have used the strategy, on the one hand, of concentrating on small ultra-thin islands where the amplitude of the quantum function oscillation is the largest and the influence of strain low. And, on the other hand, of using the WL as reference, thus getting tip-independent results. Our results show a qualitative and quantitative agreement with previous results in the literature (oscillating behavior, decay constant, phase of the beating pattern). In conclusion, the SFM/KPFM method is well-suited to determine the quantum oscillation in the work function with utmost precision.

Acknowledgements

We thank H. v. Löhneysen and M. Weides for enlightening discussions. Funding: Financial support from the European Research Council through the Starting Grant NANOCONTACTS (No. ERC 2009-Stg 239838) and from the Ministry of Science, Research and Arts, Baden-Wuerttemberg, in the framework of its Brigitte-Schlieben-Lange program is gratefully acknowledged.

References

1 F. K. Schulte, *Surf. Sci.*, 1976, **55**, 427–444.
2 T. C. Chiang, *Surf. Sci. Rep.*, 2000, **39**, 181–235.
3 M. Milun, P. Pervan and D. P. Woodruff, *Rep. Prog. Phys.*, 2002, **65**, 99–141.
4 P. Czoschke, H. Hong, L. Basile and T.-C. Chiang, *Phys. Rev. B: Condens. Matter*, 2005, **72**, 075402.
5 M. Jałochowski and E. Bauer, *Phys. Rev. B: Condens. Matter*, 1988, **38**, 5272–5280.
6 Y. Guo, Y.-F. Zhang, X.-Y. Bao, T.-Z. Han, Z. Tang, L.-X. Zhang, W.-G. Zhu, E. G. Wang, Q. Niu, Z. Q. Qiu, J.-F. Jia, Z.-X. Zhao and Q.-K. Xue, *Science*, 2004, **306**, 1915–1917.
7 D. Eom, S. Qin, M. Y. Chou and C. K. Shih, *Phys. Rev. Lett.*, 2006, **96**, 027005.
8 X. Ma, P. Jiang, Y. Qi, J. Jia, Y. Yang, W. Duan, W.-X. Li, X. Bao, S. B. Zhang and Q.-K. Xue, *Proc. Natl. Acad. Sci. U. S. A.*, 2007, **104**, 920–9208.
9 X. Liu, C.-Z. Wang, M. Hupalo, H.-Q. Lin, K.-M. Ho and M. C. Tringides, *Phys. Rev. B: Condens. Matter*, 2014, **89**, 041401(R).
10 Y. Qi, X. Ma, P. Jiang, S. H. Ji, Y. S. Fu, J. F. Jia, Q. K. Xue and S. B. Zhang, *Appl. Phys. Lett.*, 2007, **90**, 013109.
11 J. Kim, S. Qin, W. Yao, Q. Niu, M. Y. Chou and C. K. Shih, *Proc. Natl. Acad. Sci. U. S. A.*, 2010, **107**, 12761–12765.
12 R. Otero, A. L. Vázquez de Parga and R. Miranda, *Phys. Rev. B: Condens. Matter*, 2002, **66**, 115401.
13 M. Becker and R. Berndt, *Appl. Phys. Lett.*, 2010, **96**, 033112.
14 M. Hupalo, S. Kremmer, V. Yeh, L. Berbil-Bautista, E. Abram and M. C. Tringides, *Surf. Sci.*, 2001, **493**, 526–538.

15 C. M. Wei and M. Y. Chou, *Phys. Rev. B: Condens. Matter*, 2002, **66**, 233408.
16 L. Wang, X. C. Ma, P. Jiang, Y. S. Fu, S. H. Ji, J. F. Jia and Q. K. Xue, *J. Phys.: Condens. Matter*, 2007, **19**, 306002.
17 P. S. Kirchmann, M. Wolf, J. H. Dil, K. Horn and U. Bovensiepen, *Phys. Rev. B: Condens. Matter*, 2007, **76**, 075406.
18 Y.-F. Zhang, J.-F. Jia, T.-Z. Han, Z. Tang, Q.-T. Shen, Y. Guo, Z. Q. Qiu and Q.-K. Xue, *Phys. Rev. Lett.*, 2005, **95**, 096802.
19 P. Czoschke, H. Hong, L. Basile and T. C. Chiang, *Phys. Rev. Lett.*, 2004, **93**, 036103.
20 T. Miller, M. Y. Chou and T.-C. Chiang, *Phys. Rev. Lett.*, 2009, **102**, 236803.
21 M. Nonnenmacher, M. P. Oboyle and H. K. Wickramasinghe, *Appl. Phys. Lett.*, 1991, **58**, 2921–2923.
22 S. A. Burke, J. M. LeDue, Y. Miyahara, J. M. Topple, S. Fostner and P. Grütter, *Nanotechnology*, 2009, **20**, 264012.
23 J. L. Neff, P. Milde, C. Pérez León, M. D. Kundrat, C. R. Jacob, L. Eng and R. Hoffmann-Vogel, *ACS Nano*, 2014, **8**, 3294–3301.
24 C. Pérez León, H. Drees, S. M. Wippermann, M. Marz and R. Hoffmann-Vogel, *J. Phys. Chem. Lett.*, 2016, **7**, 426–430.
25 R. Feng, E. H. Conrad, M. C. Tringides, C. Kim and P. F. Miceli, *Appl. Phys. Lett.*, 2004, **85**, 3866–3868.
26 C. Barth and C. R. Henry, *Phys. Rev. Lett.*, 2007, **98**, 136804.
27 H.-Q. Mao, N. Li, X. Chen and Q.-K. Xue, *Chin. Phys. Lett.*, 2012, **29**, 066802.
28 P. A. Thiel, M. Shen, D.-J. Liu and J. W. Evans, *J. Phys. Chem. C*, 2009, **113**, 5047–5067.
29 S. Sadewasser and M. C. Lux-Steiner, *Phys. Rev. Lett.*, 2003, **91**, 266101.
30 I. B. Altfeder, K. A. Matveev and D. M. Chen, *Phys. Rev. Lett.*, 1997, **78**, 2815–2818.
31 Y. Jia, B. Wu, C. Li, T. L. Einstein, H. H. Weitering and Z. Zhang, *Phys. Rev. Lett.*, 2010, **105**, 066101.
32 J. Kim, C. Zhang, J. Kim, H. Gao, M.-Y. Chou and C.-K. Shih, *Phys. Rev. B: Condens. Matter*, 2013, **87**, 245432.
33 Y. Jia, B. Wu, H. H. Weitering and Z. Zhang, *Phys. Rev. B: Condens. Matter*, 2006, **74**, 035433.
34 S. Pan, Q. Liu, F. Ming, K. Wang and X. Xiao, *J. Phys.: Condens. Matter*, 2011, **23**, 485001.
35 M. Liu, Y. Han, L. Tang, J.-F. Jia, Q.-K. Xue and F. Liu, *Phys. Rev. B: Condens. Matter*, 2012, **86**, 125427.